








Some Improvements of a Visco-Plastic Constitutive Model for Snow

Gianmarco Vallero^(✉) , Monica Barbero , Fabrizio Barpi ,
Mauro Borri-Brunetto , and Valerio De Biagi 

Politecnico di Torino, 10129 Turin, TO, Italy
gianmarco.vallero@polito.it

Abstract. Snow is a peculiar example of a granular and low density geomaterial that exists at environmental conditions very close to its melting point. Once snowflakes deposit onto the ground, they start to evolve under the effect of both temperature and stress conditions (i.e., snow metamorphism): the result is therefore a complex three-phase material where an ice skeleton (i.e., snow microstructure) is encompassed by voids filled with air and liquid water. From a mechanical point of view, seasonal snow is therefore characterized by bonding/degradation processes between grains, large inelastic deformations and rate-sensitivity. Moreover, in nature, snow can be found in different shapes and structures having significant differences in terms of mechanical strength and physical properties. Therefore, the need for a constitutive model that can be representative of different types and conditions of snow is of paramount importance. Snow mechanics is indeed a topic of wide interest for many application fields, such as: design and management of structures and infrastructure in cold environments; study of new materials for winter sports and leisure activities; avalanche forecast, release and propagation, etc.

In this work, we report on some improvements to an existing constitutive model for snow that was developed in the framework of the nonlinear theory of elasto-visco-plasticity. The numerical implementation was achieved via a fully implicit integration algorithm and a local nonlinear resolving scheme. Finally, some preliminary results are described referring to literature experimental data on snow.

Keywords: Snow mechanics · Finite Element Analysis · Constitutive modelling

1 Introduction

Snow is a natural material composed of an ice skeleton encompassed by voids filled with liquid water and water vapour [1]. The mechanical behaviour of this heterogeneous material depends on a number of factors, such as: snow microstructure, thermal metamorphisms, water changes of phase, environmental conditions, loading rate, etc. [2, 3]. All these aspects make the modelling of the mechanical behaviour of snow a complex and difficult task. However, snow mechanics is crucial to address many interesting problems such as the stability of mountain snowpacks, the design of structures and infrastructures in cold environments, the safety of humans and goods in snow covered areas, the assessment of social and physical risk due to snow avalanches, etc. [4–6].

In the framework of Continuum Mechanics, the available snow models are generally developed with reference to the elasto-plastic (EP) theory to model both laboratory experiments and, on some occasions, on-site tests [7]. Nevertheless, available models are generally tailored to some specific types of snow (i.e., rounded grains, faceted crystals, etc.) and cannot be adopted for general purposes [8, 9]. Moreover, many models do not consider the bonding and sintering effects, the viscosity of the ice skeleton, the rate-sensitivity of the material, the volumetric collapse of the weak layer, etc.

In this work, we report on some significant improvements to the EP constitutive model originally proposed by [10] and [11]. Therefore, the improved model is based on: i) the framework and a new integration of the existing model [11], and ii) a new flexible yield locus and visco-plastic strain potential. At the moment, the model is able to quantitatively reproduce many experimental data available in the international scientific literature for dry snow with rounded grains [12–14]. The main outcome of this work is to build a solid basis for a new model that will be able to reproduce the behaviour of different types of snow: rounded and cohesive snow (typical of the snow slab) as well as faceted and low resistance snow (weak layer snow).

2 The Model

The improved model proposed in this work lies on the hypotheses of continuity, homogeneity and isotropy, and is based on the following three key points:

- the general framework of the constitutive model for snow developed by [11] which includes a valuable analytical law for sintering and degradation;
- the overstress theory of viscosity proposed by [15] and then modified by [10] to account also for the presence of irrecoverable strains inside the elastic region;
- a new formulation for the yield locus and the visco-plastic strain potential.

The temperature is assumed to be constant during the simulations, therefore, the model is purely mechanical. Here, we follow the small strain theory and the strain rate tensor is additively decomposed to produce the following usual stress-strain vector relationship:

$$\dot{\boldsymbol{\sigma}} = \mathbf{D}_{\text{el}}(\dot{\boldsymbol{\epsilon}} - \dot{\boldsymbol{\epsilon}}^{\text{VP}}) \quad (1)$$

where $\boldsymbol{\sigma}$ is the stress tensor (written in Voigt's notation), $\dot{\boldsymbol{\epsilon}}$ is the total strain rate vector, $\dot{\boldsymbol{\epsilon}}^{\text{VP}}$ is the visco-plastic strain rate vector, and \mathbf{D}_{el} is the elastic stiffness matrix. The elastic matrix can be written with reference to the two Lamé coefficients A and B :

$$\mathbf{D}_{\text{el}} = \begin{pmatrix} A & B & B & 0 & 0 & 0 \\ B & A & B & 0 & 0 & 0 \\ B & B & A & 0 & 0 & 0 \\ 0 & 0 & 0 & G & 0 & 0 \\ 0 & 0 & 0 & 0 & G & 0 \\ 0 & 0 & 0 & 0 & 0 & G \end{pmatrix} \quad (2)$$

where: $A = -\frac{\nu p}{k} + \frac{4}{3}G$, $B = -\frac{\nu p}{k} - \frac{2}{3}G$, ν is the specific volume, p is the mean volumetric stress, k is the elastic compressibility, and G is the shear modulus. In the

following subsections a brief description of the main theoretical aspects of the model is presented.

2.1 Yield Locus and Irreversible Strain Potential

In the present work, a new and unsymmetrical yield surface capable of changing its shape in the meridian plane is proposed and tested. The need for such a surface is linked to the generality that an arbitrary shape can provide to the model and the capability of the surface to deform and change its shape following specific numerical requirements and/or experimental findings. The starting point for the new surface is the snow version of the Modified Cam Clay proposed by [10]:

$$f_C(p, q) = \frac{1}{p_{atm}^2} \left\{ q^2 - M^2 \left[p(p_0 + p_m - p_t) + p_t(p_0 + p_m) - p^2 \right] \right\} \quad (3)$$

where q is the equivalent Mises stress, p_0 is the mean consolidation stress for unbonded snow, p_{atm} is the mean atmospheric pressure, M is the slope of the critical state line, p_m and p_t are the two additional strength parameters (always positive) measuring the bonding of the snow in compression and tension, respectively. Following [8] and [11] we assumed their ratio defined by a constant: $p_t = \chi p_m$. Following the theoretical procedure proposed by [16], we introduced a function $\Gamma(p)$ that modulates the invariant q of the original surface allowing the locus to be flexible and obtaining shapes ranging from bullet-like to drop-like ones:

$$f(p, q) = \frac{1}{p_{atm}^2} \left\{ q^2 \Gamma(p) - M^2 \left[p(p_0 + p_m - p_t) + p_t(p_0 + p_m) - p^2 \right] \right\} \quad (4)$$

Imposing that the apex of the curve has the coordinates $(\alpha(p_0 + p_m), \alpha M(p_0 + p_m))$, the analytical expression of the new yield function $f(p, q)$ is the following:

$$f(p, q) = \frac{1}{p_{atm}^2} \left\{ q^2 - 4\alpha^2 M^2 (p_0 + p_m)^3 \frac{(\alpha - 1)(p - p_t)(p + p_0 + p_m)[p_t + \alpha(p_0 + p_m)]}{\{-p(p_0 + p_m - p_t) + 2p(p_0 + p_m)\alpha + (p_0 + p_m)[-(\alpha - 2)p_t + (p_0 + p_m)\alpha]\}^2} \right\} \quad (5)$$

where α and M are the only two shape parameters (Fig. 1). The former parameter governs the symmetry of the curve around a vertical axis while the latter describes the slope of the critical state line and therefore measures the size of the yield curve. Suggested values for α are in the range [0.15, 0.75] whereas M will be between 0.50 and 3.00 [8, 13]. In Fig. 2 a short parametric analysis of the effect of both α and M is reported.

From a mathematical point of view, the function $f = 0$ describes a curve which is simply convex and smooth in any point of the $p - q$ plane. The convexity could therefore be lost for some value of f greater than 0. Thus, a similar expression for the visco-plastic strain potential is used to obtain the direction of the visco-plastic strains:

$$g(p, q) = q^2 - 4\alpha^2 M^2 p_{g0}^3 \frac{(\alpha - 1)(p - p_{gt})(p + p_{g0})[p_{gt} + \alpha p_{g0}]}{\{-p(p_{g0} - p_{gt}) + 2\alpha p p_{g0} + p_{g0}[-(\alpha - 2)p_{gt} + \alpha p_{g0}]\}^2} \quad (6)$$

where $p_{g0} = p_0 + p_m$ and $p_{gt} = p_t$. This definition ensures that g is null for any stress state (p, q) .

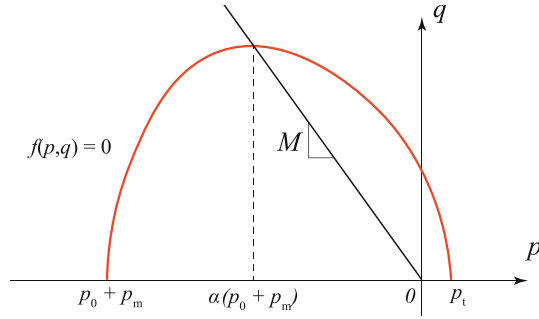


Fig. 1. Sketch of the meridian section of the yield surface proposed in this work.

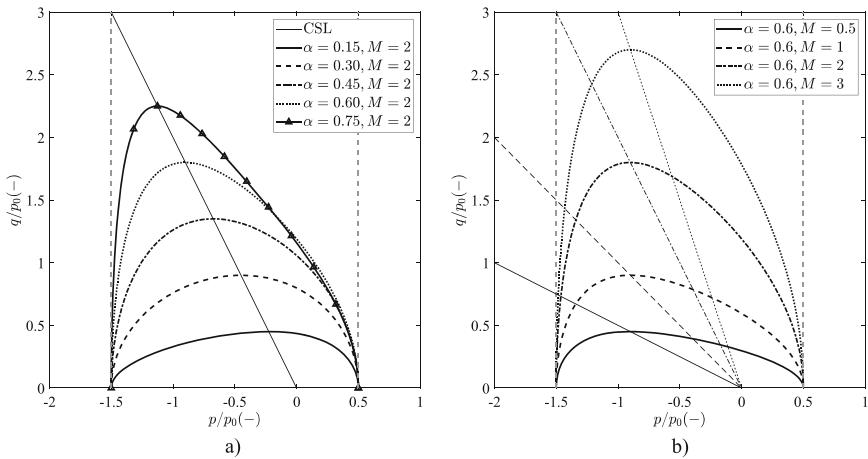


Fig. 2. Parametric analysis on the effect of the shape parameters on the meridian section of the new yield function. a) Effect of α for constant M . The elliptical shape is obtained for $\alpha = 0.475$ where, for different values, the surface progressively unsymmetric. b) Effect of M for constant α .

2.2 Viscosity and Flow Rule

A non-associative flow rule of the Perzyna type was chosen [15]. The model is modified from the original viscosity model to allow viscous-plastic irreversible strains to occur both inside and outside the yield locus. This allows to better reproduce some experimental findings where the viscous behaviour starts from the very beginning of the strain-stress history. In detail, the flow rule can be written as:

$$\dot{\epsilon}^{vp} = \bar{\psi} \phi(f) = \psi \frac{\sqrt{p^2 + q^2}}{\sqrt{3}p_0} e^{af} \left. \frac{\partial g}{\partial \sigma} \right|_{\text{norm}} \quad (7)$$

where ψ is a constitutive parameter having the dimensions of a strain rate; f is the current value of the yield function; $\left. \frac{\partial g}{\partial \sigma} \right|_{\text{norm}}$ is the normalized first derivative (unit vector) of the visco-plastic potential g ; $\bar{\psi}$ is the fluidity parameter defining the rate at which the

irrecoverable strains occurs; $\phi(f)$ is the viscous nucleus relating the strain amount to the distance between the stress state and the yield surface $f = 0$. For the sake of conciseness, the dimensionless parameter β is defined as follows [10]:

$$\beta = \psi \frac{\sqrt{p^2 + q^2}}{\sqrt{3}p_0} e^{af} \tag{8}$$

2.3 Sintering and Hardening Laws

The sintering law adopted in this work is the same proposed by Cresseri (2005) based on literature data, for which we refer to their work for further information [10]. The current degree of sintering is given as:

$$S = S_0 \left[1 - \tanh \left(C \int_0^t \sqrt{(\dot{\epsilon}_v^{vp})^2 + (\dot{\epsilon}_d^{vp})^2} dt \right) \right] \tag{9}$$

where S_0 is the degree of sintering for the unbonded material, C is a material parameter, $\dot{\epsilon}_v^{vp}$ are $\dot{\epsilon}_d^{vp}$ the volumetric and deviatoric parts of the strain rate tensor, respectively. The amount of sintering is finally related to the additional pressure in compression (p_m) with the following rate relation, in which π_m is a constitutive parameter and is b_{max} the maximum ratio between the neck size and the radius of the snow grain:

$$\dot{p}_m = \pi_m b_{max} \dot{S} \tag{10}$$

The usual volumetric hardening law of the Modified Cam Clay is used to describe the evolution of the mean consolidation stress:

$$\dot{p}_0 = -\frac{v}{\lambda - k} p_0 \dot{\epsilon}_v^{vp} \tag{11}$$

3 Numerical Implementation and Results

The proposed model is composed of a system of 10 nonlinear differential equations to be solved together at any time increment. The constitutive equations are the following:

$$\frac{1}{Z_1} \left(\dot{\sigma} - \mathbf{D}_{el} \dot{\epsilon} + \mathbf{D}_{el} \beta \frac{\partial g}{\partial \sigma} \Big|_{norm} \right) = 0 \tag{12}$$

$$\frac{1}{Z_2} g(\sigma) = 0 \tag{13}$$

$$\frac{1}{Z_1} \left(\dot{p}_0 + \frac{v}{\lambda - k} p_0 \dot{\epsilon}_v^{vp} \right) = 0 \tag{14}$$

$$\dot{p}_m - \pi_m b_{max} \dot{S} = 0 \tag{15}$$

$$S - S_0 \left[1 - \tanh \left(C \int_0^t \sqrt{(\dot{\epsilon}_v^{vp})^2 + (\dot{\epsilon}_d^{vp})^2} dt \right) \right] = 0 \quad (16)$$

where the Eq. (12) represents a vector relation of 6 component. Z_0 and Z_1 are two normalizing parameters [11].

The equations were integrated over time by using a fully implicit backward Euler method and the local problem of solving the nonlinear 10-dimension system was solved with an iterative scheme based on the Powell's hybrid method (i.e., a generalized Newton-Raphson method) [17]. The solution of both the general and local problems has been implemented into the UMAT format (written in Fortran 77) for the Abaqus/Standard Finite Element code [18].

To test the capability of the model some numerical analyses were performed on a single finite element with reference to creep tests (Fig. 3a), isotropic compression tests (Fig. 3b) and triaxial compression tests (Fig. 4a and 4b). In general, the model seems able to satisfactorily reproduce the experimental tests. Some issues (related to numerical problems and lack of convergence) can be observed during the isotropic unloading (Fig. 3b) and the triaxial relaxation, especially in quick-time tests (Fig. 4b), where the numerical drop of tension is quicker than the one reported in the experimental findings. In Tables 1 and 2 the model parameters and the initial conditions used in the numerical simulations are reported, respectively.

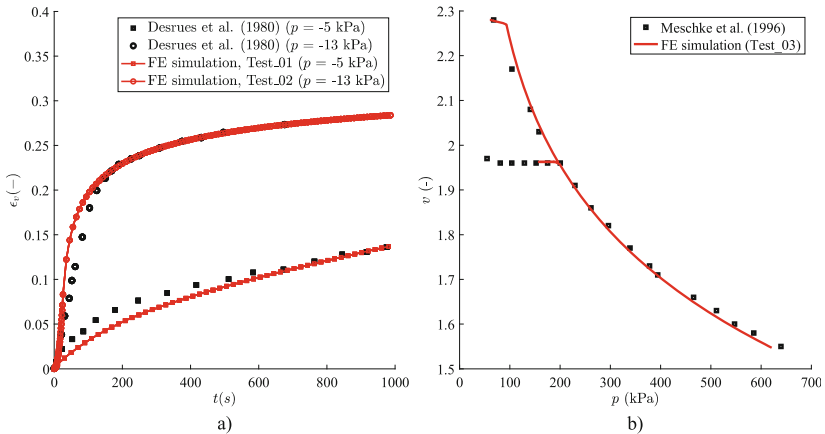


Fig. 3. Comparison between the experimental results and the numerical prediction: a) results for volumetric creep tests [12]; b) results for isotropic compression test [13].

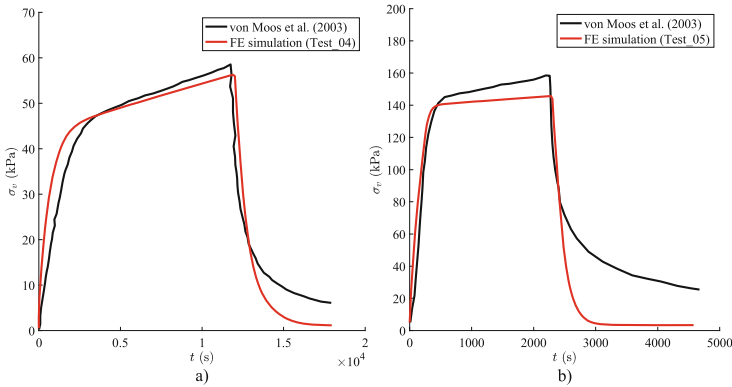


Fig. 4. Comparison between the experimental results and the numerical prediction: a) results for triaxial test in case of long-time test [14]; b) results for triaxial test in case of quick-time test [14].

Table 1. Model parameters used in the simulations.

Test ID	λ (-)	k (-)	G (kPa)	ψ (-)	a (-)	π_m (-)	χ (-)	C (-)	M (-)	α (-)
Test_01	0.35	0.02	2114	1.2e-4	16	40	0.05	0.01	2.88	0.475
Test_02	0.35	0.02	2114	1.2e-4	16	40	0.05	0.01	2.88	0.475
Test_03	0.35	0.02	12000	2.0e-7	16	40	0.05	0.01	2.88	0.475
Test_04	0.35	0.02	8000	4.2e-6	0.35	40	0.05	0.01	2.88	0.475
Test_05	0.35	0.02	20000	2.0e-5	0.35	40	0.05	0.01	2.88	0.475

Table 2. Initial conditions assumed in the simulations.

Test ID	p^0 (kPa)	p_0 (kPa)	v_0 (-)	T (°C)	r_0 (mm)
Test_01	0.0	2	4.58	-5	0.2
Test_02	0.0	2	4.58	-5	0.2
Test_03	-60.0	77	2.28	-5	0.2
Test_04	0.0	25	2.90	-12	0.118
Test_05	-5.0	100	2.44	-12	0.118

4 Discussion and Conclusions

In this work we describe an improved nonlinear visco-plastic model for snow, based on an improved version of the existing framework of the model by [11] and a new unsymmetric yield surface and irreversible strain potential. The new yield locus will be tested in the future to check its reliability and flexibility with respect to a larger collection of data. The model was implemented into the UMAT format for the FE code ABAQUS/Standard

and both a fully implicit method and a local iterative algorithm were introduced in the code. The model can reproduce satisfactorily many different laboratory findings as can be deduced in Figs. 3 and 4. Some convergence issues can be found during the unloading isotropic phase (strain control). We are planning in the next future to update the model in order to avoid numerical issues and improve its stability even in these cases. In general, the model is able to replicate both qualitatively and quantitatively the actual behavior of the snow under different stress and strain conditions. This is a significant step towards the complete development of a viscous rate-dependent model with sintering that could be used in the future to model real scale phenomena linked to snow (avalanche triggering, weak layer collapse, etc.).

References

1. Mellor, M.: Engineering properties of snow. *J. Glaciol.* **19**(81), 15–66 (1977)
2. Petrovic, J.J.: Review mechanical properties of ice and snow. *J. Mater. Sci.* **38**, 1–6 (2003)
3. Blackford, J.R.: Sintering and microstructure of ice: a review. *J. Phys. D Appl. Phys.* **40**(21), 355–385 (2007)
4. Mellor, M.: A review of basic snow mechanics. In: IAHS Publ. (eds.) *Snow Mechanics. Proceedings of the Grindelwald Symposium April 1974*, vol. 114, pp. 251–291 (1975)
5. McCallum, A., White, G.W.: Engineered pavement of snow and ice. In: 8th International Conference on Snow Engineering (2016)
6. Vallero, G., et al.: Experimental study of the shear strength of a snow-mortar interface. *Cold Reg. Sci. Technol.* **193**, 103430 (2022)
7. Podolskiy, E.A., Chambon, G., Naaim, M., Gaume, J.: A review of finite-element modelling in snow mechanics. *J. Glaciol.* **59**(218), 1189–1201 (2013)
8. Gaume, J., Gast, T., Teran, J., van Herwijnen, A., Jiang, C.: Dynamic anticrack propagation in snow. *Nat. Commun.* **9**(1), 3047 (2018)
9. Vallero, G., Barbero, M., Barpi, F., Borri-Brunetto, M., Biagi, V.: Some computational issues in the elasto-plastic modelling of snow. In: 16th Edition of the International Conference on Computational Plasticity (2021)
10. Cresseri, S.: Constitutive modelling of dry granular snow at low strain rates. PhD thesis. Politecnico di Milano, Milano (2005)
11. Cresseri, S., Genna, F., Jommi, C.: Numerical integration of an elastic–viscoplastic constitutive model for dry metamorphosed snow. *Int. J. Num. Anal. Methods Geomech.* **34**(12), 1271–1296 (2010)
12. Desrués, J., Darve, F., Flavigny, E., Navarre, J., Taillefer, A.: An incremental formulation of constitutive equations for deposited snow. *J. Glaciol.* **25**(92), 289–307 (1980)
13. Meschke, G., Liu, C., Mang, H.A.: Large strain finite-element analysis of snow. *J. Eng. Mech.* **122**(7), 591–602 (1996)
14. von Moos, M., Bartelt, P., Zweidler, A., Bleiker, E.: Triaxial tests on snow at low strain rate. Part I. Experimental device. *J. Glaciol.* **49**(164), 81–90 (2003)
15. Perzyna, P.: The constitutive equations for rate sensitive plastic materials. *Q. Appl. Math.* **20**, 321–332 (1963)
16. Panteghini, A., Lagioia, R.: An extended modified Cam-Clay yield surface for arbitrary meridional and deviatoric shapes retaining full convexity and double homothety. *Geotechnique* **68**(7), 590–601 (2018)
17. Powell, M.J.D.: A Fortran Subroutine for Solving Systems of Nonlinear Algebraic Equations. United Kingdom (1968)
18. Abaqus, G.: AA.VV. Abaqus 6.11. Dassault Systemes Simulia Corporation, Providence, RI, USA (2011)